Low-lying dipole excitations in vibrational nuclei: The Cd isotopic chain studied in photon scattering experiments

C. Kohstall,[1] D. Belic,[1,*] P. von Brentano,[2] C. Fransen,[2] A. Gade,[2,†] R.-D. Herzberg,[2,‡] J. Jolie,[2] U. Kneissl,[1] A. Linnemann,[2] A. Nord,[1,*] N. Pietralla,[2,§] H. H. Pitz,[1] M. Scheck,[1] F. Stedile,[1] V. Werner,[2,¶] and S. W. Yates[3]

[1]*Institut für Strahlenphysik, Universität Stuttgart, D-70569 Stuttgart, Germany*

[2]*Institut für Kernphysik, Universität zu Köln, D-50937 Köln, Germany*

[3]*Departments of Chemistry and Physics & Astronomy, University of Kentucky, Lexington, Kentucky 40506-0055, USA*

(Received 29 April 2005; published 20 September 2005)

High-resolution nuclear resonance fluorescence experiments (NRF) were performed on ^{110,111,112,114,116}Cd at the bremsstrahlung facility of the 4.3-MV Dynamitron accelerator in Stuttgart to study the low-lying dipole strength distributions in these vibrational nuclei. Numerous excited states, most of them previously unknown, were observed in the excitation energy range up to 4 MeV. Detailed spectroscopic information has been obtained on excitation energies, spins, decay widths, decay branchings, and transition probabilities. For states in the even-even isotopes ^{110,112,114,116}Cd, parities could be assigned from linear polarization measurements. Together with our previous results for ^{108,112,113,114}Cd from NRF studies without polarization measurements, systematics was established for the dipole strength distributions of the stable nuclei within the Cd isotopic chain. The results are discussed with respect to the systematics of $E1$ two-phonon excitations and mixed-symmetry states in even-even nuclei near the $Z = 50$ shell closure and the fragmentation of these excitation modes in the odd-mass Cd isotopes.

DOI: 10.1103/PhysRevC.72.034302 PACS number(s): 25.20.Dc, 21.10.Re, 23.20.Lv, 27.60.+j

I. INTRODUCTION

The elements in the $Z = 50$ region are particularly favorable for comprehensive nuclear structure studies, because their many stable isotopes allow systematic investigations of the evolution of different nuclear modes of excitation.

The $_{48}$Cd nuclei (6 stable even-A isotopes) have been considered as excellent examples of vibrational behavior; however, the $(2^+ \otimes 2^+)$ two-phonon triplet (with spins 0^+, 2^+, and 4^+) intermingles with additional 0^+, 2^+, and 4^+ "intruder" states formed by two-proton excitations across the $Z = 50$ shell [1–8]. The shape coexisting intruders, which exhibit moderately deformed structures, mix with normal vibrational states, thus significantly altering the properties of the expected multiphonon multiplets [9–12].

During the past decade, the Cd isotopes have emerged as *the* laboratory for the study of multiphonon excitations, such as the three-quadrupole-phonon [3,13–17] and mixed quadrupole-octupole excitations of the type $(2^+ \otimes 3^-)$ [5,14,18–20]. Complete quadrupole-octupole quintuplets were first observed in nuclei near the $N = 82$ shell closure [21,22], but have now been established in the Cd isotopes ^{108}Cd [6], ^{112}Cd [20], and ^{114}Cd [18].

Because of the diversity of excitation modes, a large variety of nuclear probes and spectroscopic tools have been applied to study the nuclear structure of these interesting nuclei. These include classical techniques such as Coulomb excitation [23], transfer reactions [24], (n, γ)-capture reactions [19,24], inelastic scattering of polarised light particles [25], β-decay studies [26–28], and, in particular, nonselective reactions such as (light-ion,x$n\gamma$)-fusion reactions, e.g., $(\alpha, 2n\,\gamma)$ [4,9,14,19], and inelastic neutron scattering (INS) [7,15–18,20,29,30]. In the two latter types of experiments γ-ray spectroscopic coincidence techniques were applied to construct the level schemes, and lifetimes, which are crucial for the interpretation, were measured using the Doppler shift attenuation method (DSAM).

The wealth of experimental data for the Cd isotopes tempted in the past to regard these nuclei as appropriate candidates, within the concept of a "complete spectroscopy," to provide a complete set of excited levels, at least in a limited range of excitation energies and a certain spin window [31,32].

In view of previous comprehensive studies of the various Cd isotopes it is appropriate to ask what additional information can be learned from photon-scattering experiments. It is well known that real photons represent a highly spin-selective probe. Because of the low transfer of momentum in photon scattering, dipole excitations (both $E1$ and $M1$) are induced predominantly, with to a lesser extent electric quadrupole transitions ($E2$). Therefore, even in ranges of excitation energies of high total level density the corresponding photoexcited levels can be investigated with high sensitivity. Spins can easily be

*Present address: Agilent Technologies, D-71034 Böblingen, Germany.

†Present address: NSCL, Michigan State University, East Lansing, MI 483824, USA.

‡Permanent address: Oliver Lodge Laboratory, University of Liverpool, Liverpool L69 7ZE, UK.

§Present address: Department of Physics and Astronomy, State University of New York, Stony Brook, NY-11794-3800, USA.

¶Present address: Wright Nuclear Structure Laboratory, Yale University, New Haven, CT 06520-812124, USA.

assigned (for even-even nuclei) from the angular distributions measured in photon scattering experiments. Parities can be determined too; however, time-consuming polarization measurements are required for these assignments. It should be emphasized that because of the well-known electromagnetic interaction mechanism all spectroscopic information can be extracted in a completely model-independent manner from nuclear resonance fluorescenec (NRF) experiments [33,34].

Photon-scattering experiments (NRF) are complementary to the nonselective inelastic neutron scattering technique (INS) in many respects. In INS, states with spins up to about $6\hbar$ can be excited in even-even nuclei, their spins are inferred from the measured excitation functions and angular distributions. In NRF, only states with spins 1 or 2 $\hbar$ can be populated and their spins are easily determined from the scattering intensities measured by two detectors installed at scattering angles of 90° and 127° with respect to the incident photon beam. As already mentioned, in INS lifetimes τ are measured directly using DSAM techniques. Conversely, decay widths Γ are determined in NRF from the scattering intensities. Both quantities are connected via the uncertainty relation, $\Gamma = \hbar/\tau$. Therefore, in cases where the lifetime is too short to be measured by DSAM the width is large and can be determined best in NRF experiments.

Dipole excitations of particular interest in even-even nuclei near shell closures are $E1$ two-phonon excitations to the spin 1 member of the quadrupole-octupole-coupled quintuplet ($1^-\ldots.\,5^-$). These $E1$ transitions have been observed in numerous nuclei near shell closures (see Ref. [35]) in systematic NRF studies. The observed systematics of strengths and decay branchings were interpreted as an evidence of core polarization. The best examples of such enhanced $E1$ two-phonon excitations are 1^- states in the magic Sn isotopes ($Z = 50$), as observed in our previous NRF experiments [36]. Therefore, it was of special interest to investigate the neighboring Cd isotopes ($Z = 48$).

Other general types of dipole modes in nuclei near closed shells are $M1$ excitations to the so-called mixed-symmetry states [18], as found and investigated in particular in nuclei near the $N = 50$ shell closure [37–40]. These studies demonstrated the importance of the combination of different spectroscopic techniques as INS, NRF, β-decay, and classical (γ, γ) coincidence techniques [41].

The aim of the present investigations was to establish a broad systematics of the above mentioned $E1$ and $M1$ excitations in the even-A Cd isotopes. Therefore, our previous NRF studies of ^{108,112,113,114}Cd [42–44] without polarization measurements were completed and extended by systematic experiments on ^{110,112,114,116}Cd, including linear polarization measurements for the crucial parity determinations. In addition, the fragmentation of the dipole modes in the neighboring odd-mass isotopes was studied in ^{111}Cd in comparison to our previous investigations of ^{113}Cd [32,44], where the knowledge of the low-lying level scheme, furthermore, is of astrophysical relevance [32,45].

After a short explanation of the NRF technique and description of the experimental setups in Sec. II, the results are presented in Sec. III and discussed in Sec. IV.

II. EXPERIMENTAL METHOD

A. The nuclear resonance fluorescence technique

Nuclear resonance fluorescence, photon scattering from bound nuclear states, represents a well-established outstanding tool for studying low-lying dipole excitations in heavy nuclei [33]. In NRF experiments using continuous bremsstrahlung photons the total scattering intensity $I_{S,f}$, the cross section integrated over one resonance and the full solid angle,

$$I_{S,f} = g \left(\pi \frac{\hbar c}{E_x}\right)^2 \frac{\Gamma_0 \Gamma_f}{\Gamma} \tag{1}$$

is determined absolutely from the spectra of scattered photons. Here Γ_0, Γ_f, and Γ are the decay widths of the excited state with spin J to the ground state with spin J_0, the final level, and the total level width, respectively. The so-called spin factor, $g = (2J + 1)/(2J_0 + 1)$, is equal to 3 in the case of dipole excitations in even-even nuclei. The quantity $g\,\Gamma_0$ is proportional to the reduced excitation probabilities $B(\Pi L, E_x) \uparrow = B(\Pi L; J_0 \rightarrow J(E_x))$, ($\Pi = E$ or M) and given by the following:

$$g\,\Gamma_0 = 8\pi \sum_{\Pi L=1}^{\infty} \frac{L+1}{L[(2L+1)!!]^2} \left(\frac{E_x}{\hbar c}\right)^{2L+1} B(\Pi L, E_x) \uparrow \tag{2}$$

The following numerical relations are useful in practice for electric or magnetic dipole excitations, respectively:

$$B(E1) \uparrow = 0.955\, \frac{g\Gamma_0}{E_x^3} [10^{-3}\,\mathrm{e^2 fm^2}] \tag{3}$$

$$B(M1) \uparrow = 0.0864\, \frac{g\Gamma_0}{E_x^3} [\mu_N^2]. \tag{4}$$

Here the excitation energies E_x are in mega-electron-volts and the ground-state transition widths Γ_0 in milli-electron-volts.

Measurements of the angular distributions of the scattered photons provide the spins J of the photoexcited levels (unambiguously in the case of even-even nuclei). The most favorable intensity ratio $W(\Theta = 90^\circ)/W(\Theta = 127^\circ)$ is 0.734 and 2.28 for pure dipole and quadrupole transitions, respectively. These values are only slightly modified by realistic geometries and the finite solid angles of the detectors.

For parity assignments, which are crucial for the interpretation of the results, the linear polarization of the scattered photons has to be measured (e.g., by using Compton polarimeters). Parity information then is obtained from the measured azimuthal asymmetry ε,

$$\varepsilon = \frac{N_\perp - N_\parallel}{N_\perp + N_\parallel} = P_\gamma\, Q \tag{5}$$

where $N_\perp$ and $N_\parallel$ represent the rates of Compton-scattered events perpendicular and parallel to the NRF scattering plane, defined by the directions of the incoming photon beam and the scattered photons, respectively. The asymmetry ε is given by the product of the polarization sensitivity Q of the polarimeter and the degree of polarization P_γ of the scattered photons. At a scattering angle of $\Theta = 90^\circ$ to the beam axis, the polarization P_γ has maximal values and is -1 or $+1$ for pure $E1$ and

$M1$ excitations, respectively (0–1–0 spin sequences). The sign of the asymmetry ε then directly provides the parity.

Unfortunately, in the case of odd-mass target nuclei the angular distributions of the scattered photons are nearly isotropic. Therefore, in general, unambiguous spin assignments to the photoexcited states are not possible, particularly for isotopes with large ground-state spins. As a consequence of the vanishing anisotropies of the angular distributions, the degree of linear polarization of the scattered photons is rather small, and no parity assignments are possible from linear polarization measurements. For comparison of the strengths observed in odd-mass isotopes with those in even-even nuclei, the quantity $g\,\Gamma_0^{\mathrm{red}}$ is introduced

$$g\Gamma_0^{\mathrm{red}} = g\,\frac{\Gamma_0}{E_x^3}, \tag{6}$$

which can be deduced from the measured scattering intensities and is proportional to the reduced dipole excitation probabilities $B(E1)\uparrow$ or $B(M1)\uparrow$ [see Eqs. (3) and (4)].

Decay branchings of the photoexcited states to lower lying excited levels can be determined applying the Ritz combination rules. In the present work the applied criteria are an agreement of the sum energies and the level energies within 1 keV and the observation in at least two spectra taken at different scattering angles. The branching ratio R_{expt} relative to the ground-state decay is defined as follows:

$$R_{\mathrm{expt}} = \frac{B(\Pi L;\, J \to J_f)}{B(\Pi L;\, J \to J_0)} = \frac{\Gamma_f}{\Gamma_0}\,\frac{E_{\gamma J_0}^3}{E_{\gamma J_f}^3}. \tag{7}$$

The formalism of NRF experiments is described in greater detail elsewhere [33,34].

B. Experimental setups

The present NRF experiments on ^{110,111,112,114,116}Cd were performed at the bremsstrahlung facility of the 4.3-MV Stuttgart Dynamitron accelerator and extend our previous studies of ^{108,112,113,114}Cd [42–44]. In the present experiments on ^{110,112,114,116}Cd the linear polarizations of the scattered photons were measured using two single crystal Compton polarimeters simultaneously. The DC electron currents in the present experiments had to be limited to about 250 μA, because of the thermal capacity of the gold radiator target. In Table I beam parameters and measuring times for all Stuttgart NRF experiments on the Cd isotopes are summarized. For all experiments, isotopically enriched targets were available. The compositions, total masses, and major impurities ($\geqslant$0.5%) are given in Table II. For the polarization measurements, enriched target materials in quantities of 4–8 g were available. These large targets, together with the operation of *two* single crystal Compton polarimeters and running times on the order of 2–3.5 weeks, permitted parity assignments for the stronger transitions. The NRF targets were sandwiched between ^{27}Al disks that served for the photon flux calibration [48].

At the Stuttgart bremsstrahlung [33] facility, two setups can be operated simultaneously. At the first site the energy spectra and angular distributions of the scattered photons were detected by three high-resolution Ge(HP) γ-ray spectrometers installed at angles of about 90°, 127°, and 150°

TABLE I. Beam parameters and measuring times.

Isotope	End point energy [MeV]	Electron current on target [μA]	Measuring time [h]
^{110}Cd	4.05	250	42[a]
	4.05	260	345[b]
	3.80	265	125[b]
^{111}Cd	4.05	250	132[a]
^{112}Cd	4.00	230	69[a]
	4.10	200	419[b]
	3.15	320	211[b]
^{113}Cd	4.05	230	64[a]
	3.05	250	60[a]
^{114}Cd	4.05	250	81[a]
	4.05	260	596[b]
^{116}Cd	4.05	250	319[b]
	2.70	360	61[b]

[a]Performed at the first NRF site (cross section and angular distribution measurements).
[b]Performed at the second NRF site (in addition, polarization measurements with two Compton polarimeters).

with respect to the incoming bremsstrahlung beam. Each of the detectors had an efficiency ϵ of about 100% relative to a standard 7.6 × 7.6 cm NaI(Tl) detector. The energy resolutions were typically about 2 keV at a photon energies of 1.3 MeV and about 3 keV at 3 MeV. Temporarily the detector at 127° was surrounded additionally by a bismuth-germanate (BGO) anti-Compton shield to improve its response function. With this arrangement the peak-to-background ratio could be enhanced by a factor of about 2.

At the second NRF site two sectored single-crystal Ge Compton polarimeters (ϵ = 25 and 60%, temporarily with BGO shields) [49,50], installed at slightly backward angles of $\approx$95°, measured the linear polarization of the resonantly scattered photons and provided the parity information. The polarization sensitivities Q of the polarimeters were about 15% at photon energies of 1.5 MeV and 10% at 4 MeV [49]. An additional Ge γ-ray detector (ϵ = 38%) allowed the measurement of angular distributions at this second site also and hence the simultaneous investigation of a second target. For further experimental details, see Refs. [33,50,51].

III. RESULTS

Figure 1 represents an overview of (γ, γ') spectra of the investigated stable Cd isotopes as measured in Stuttgart NRF experiments using a bremsstrahlung beam of an end point energy of 4.1 MeV. The spectra of the newly investigated isotopes ^{110,111,116}Cd can be compared with those of the previously studied nuclei ^{108,112,113,114}Cd [42–44]. Shown is the energy region where the $E1$ two-phonon-excitations and 1^+ mixed-symmetry states are expected. Peaks attributed to the strong $E1$ excitations are marked by 1^-. Peaks labeled "^{27}Al" arise from the aluminum photon flux calibration standard. The single escape lines from the 2982-keV transition in ^{27}Al are marked "^{27}Al S.E." Lines at 2614 keV labeled "^{208}Pb" stem from background radiation of natural environmental activities. The smooth energy variation of the 1^- two phonon

TABLE II. Target compositions and specifications.

Isotope	Composition	Enrichment [%]	Total masses [mg]		Major impurities
			Target	^{27}Al	
^{110}Cd	Cd metal	95.49	1018	760	^{111}Cd (1.59%), ^{112}Cd (1.35%), ^{114}Cd (0.91%)
^{110}Cd	Cd metal	95.49	2299	2409	Same as above
^{110}Cd	Cd metal	97.25	5790		?
^{111}Cd	Cd metal	95.92	2097	760	^{112}Cd (2.16%), ^{114}Cd (0.96%)
^{112}Cd	CdO	98.17	1976	1000	^{113}Cd (0.62%), ^{114}Cd (0.52%)
^{112}Cd	Cd metal	97.92	4498	2532	^{113}Cd (0.91%), ^{114}Cd (0.78%)
^{113}Cd	Cd metal	94.58	4032	240	^{112}Cd (1.77%), ^{114}Cd (2.86%)
^{114}Cd	CdO	99.2	1854	420	—
^{114}Cd	CdO	99.2	1844	2028	—
^{114}Cd	Cd metal	99.07	3494		—
^{116}Cd	CdO	97.07	6039	1579	^{114}Cd (1.47%)

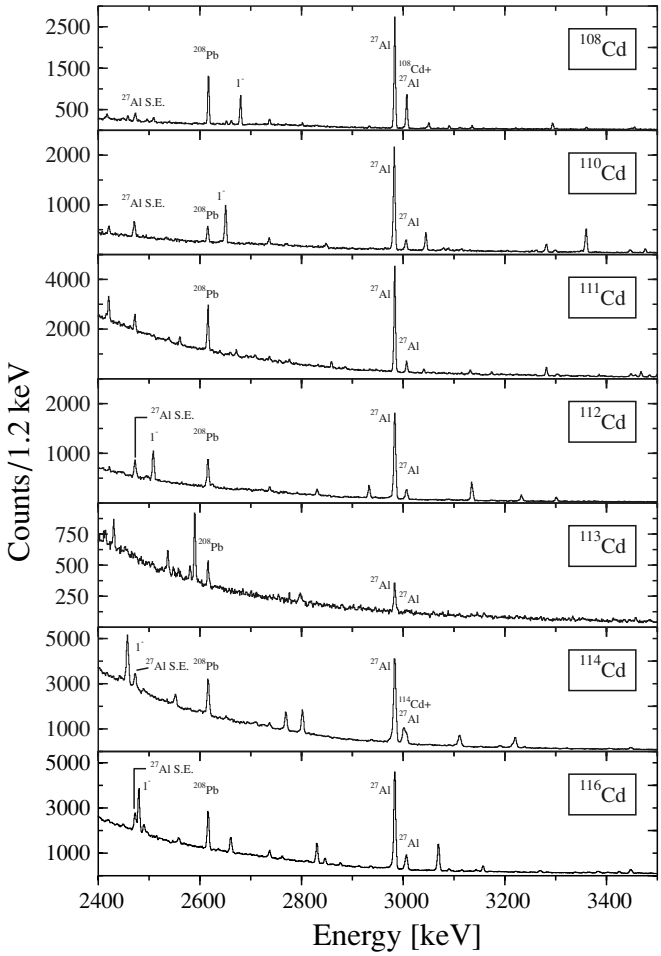

FIG. 1. (γ, γ') spectra from stable Cd isotopes investigated in Stuttgart NRF experiments with a bremsstrahlung end point energy of 4.1 MeV. Shown is the energy region where the $E1$ two-phonon excitations and 1^+ mixed symmetry states are expected. Peaks attributed to the strong $E1$ excitations are marked by 1^-. Peaks labeled ^{27}Al are from the aluminum photon flux calibration standard. Peaks marked by ^{208}Pb stem from natural environmental activities (see text).

excitations is evident. The spectrum of ^{113}Cd is dominated by a line at 2588 keV. In addition to this strong transition, an overall fragmentation of the dipole strengths in the odd-mass isotopes ^{111,113}Cd as compared to those in the neighboring even-even isotopes immediately can be noted.

As discussed above, in the case of even-even nuclei with a ground-state spin of $J_0 = 0$ unambiguous spin assignments to the excited states can be made from the intensities measured at scattering angles of 90° and 127°. As an example, in Fig. 2 the ratios $W(90°)/W(127°)$ are plotted as a function of excitation energy for the measurements on ^{110}Cd. The dotted and dashed lines correspond to the values expected for pure dipole and quadrupole excitations, respectively. For the nearly isotropic ^{27}Al radiation (open triangles) the values are consistent with unity, whereas all ^{110}Cd data points (full circles) are in agreement with the expected value for dipole

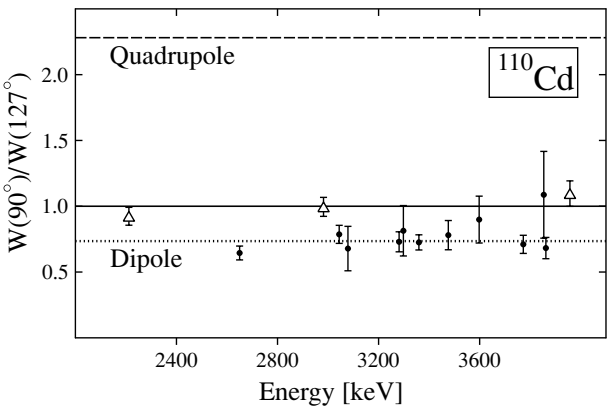

FIG. 2. Results of the angular distribution measurements in the ^{110}Cd (γ, γ') reaction. Plotted are the intensity ratios $W(90°)/W(127°)$ for the observed ground-state transitions. The dotted and dashed lines represent the expected values for dipole and quadrupole transitions (spin sequences 0–1–0 and 0–2–0), respectively. The open triangles show the ratios for the nearly isotropic transitions in ^{27}Al; the full circles give the values for the transitions in ^{110}Cd.

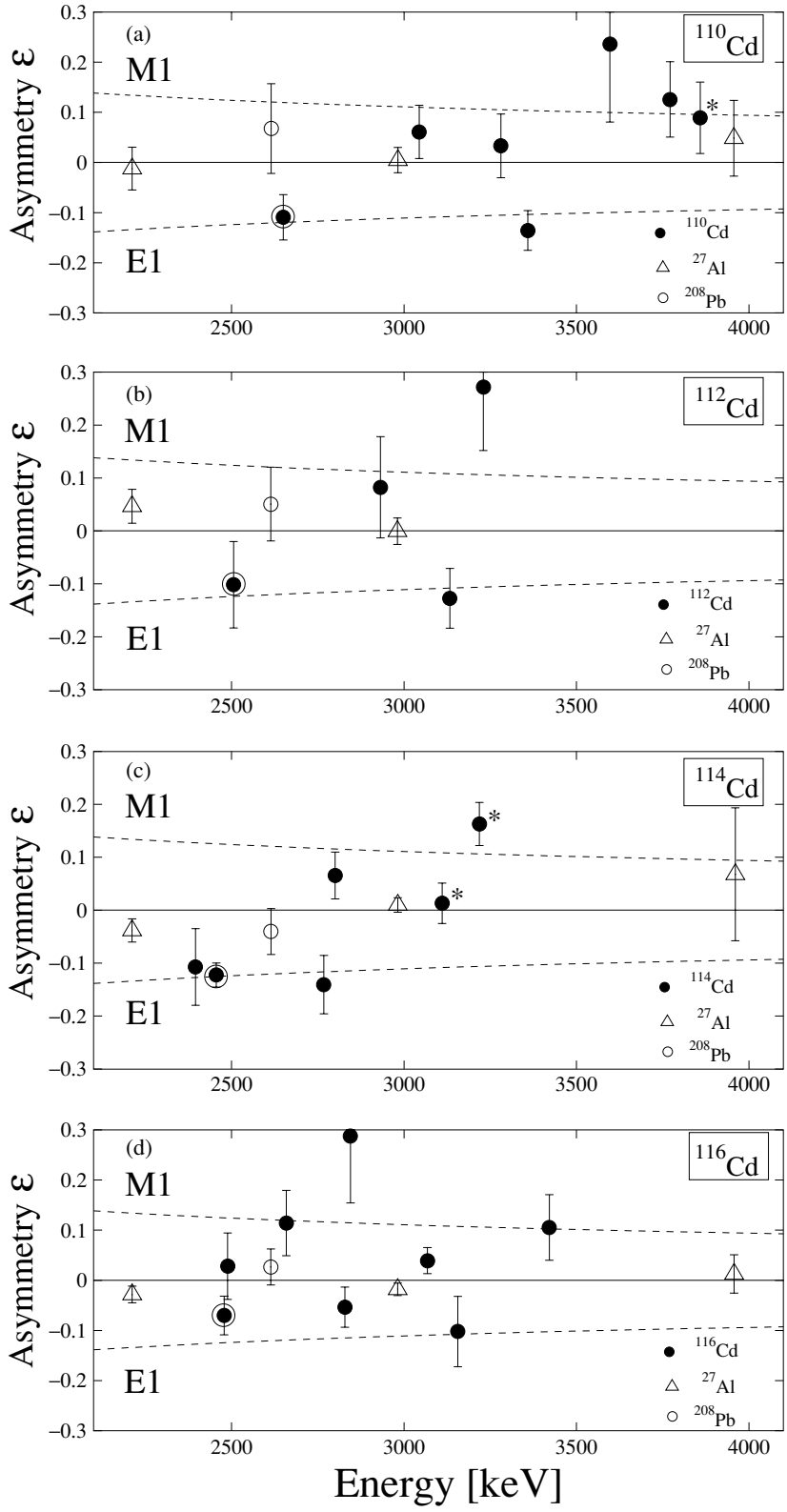

FIG. 3. Experimental results from the linear polarization measurements on ^{110}Cd, ^{112}Cd, ^{114}Cd, and ^{116}Cd. In each case, the azimuthal asymmetries ε measured (for the strongest excitations) with the Compton polarimeters together with the anticipated values for $M1$ and $E1$ transitions (dashed lines) are plotted. Full circles represent transitions in the Cd isotopes, open triangles correspond to nearly unpolarized photons from transitions in the photon flux monitor ^{27}Al, and open circles are for the unpolarized 2.614 MeV background line from ^{208}Pb. Encircled symbols label the asymmetries of the assigned $E1$ two-phonon excitations. Asterisks denote unresolvable doublets of peaks (see text).

excitations. Therefore, for all photoexcited states in ^{110}Cd the spin $J = 1$ is assigned.

The anisotropic angular distributions of photons scattered from even-even nuclei is connected with a nonzero linear polarization of the scattered photons. The sign of the linear polarization determines the parity of the transition and hence that of the excited state, because the parities of the ground states of even-even nuclei are known to be positive (see Sec. II A).

In Fig. 3 the azimuthal asymmetries ε of the even-A Cd isotopes ^{110,112,114,116}Cd, as measured by the two Compton

polarimeters for the first time in the present experiments, are depicted. The dashed lines correspond to the values for $M1$ and $E1$ transitions as expected from the calibrated polarization sensitivity of the Compton polarimeters. Positive values of ε correspond to $M1$ excitations and negative values to $E1$ transitions following the definitions of Eq. (5). Full circles belong to transitions in the Cd isotopes, open triangles correspond to nearly unpolarized photons from transitions in the photon flux monitor ^{27}Al, and open circles refer to the unpolarized 2.614 MeV background line from ^{208}Pb. The asymmetries for these unpolarized photons are in agreement with zero (within the uncertainties) demonstrating the nearly complete symmetry of the sectored single crystal Compton polarimeters. Asterisks mark unresolvable doublets of peaks, where the total asymmetries are given. The asymmetries of the expected $E1$ two-phonon excitations around 2.5 MeV are emphasized by encircled full symbols.

The results of the present experiments are summarized in numerical form in the Tables III–VII. The data for ^{108}Cd and ^{113}Cd, previously studied at Stuttgart, can be found in Refs. [42,44]. For the odd-mass isotope ^{111}Cd, the excitation energies E_x and total elastic-scattering cross sections $I_{S,0}$ are given, together with the products of the statistical factor g times the ground-state widths Γ_0, along with the reduced ground-state widths $\Gamma_0^{\rm red}$. Furthermore, the branching ratios $R_{\rm expt}$ for decay to the first excited state are quoted and the reduced excitation strengths, both $B(M1)\uparrow$ and $B(E1)\uparrow$, because no parity assignments could be made. For the even-even isotopes ^{110,112,114,116}Cd, where polarization measurements were performed, the excitation energies E_x, total elastic scattering cross sections $I_{S,0}$, branching ratios $R_{\rm expt}$ for the decay to the first excited states, and the measured azimuthal asymmetries ε are given. The deduced spins and parities J^π and the ground-state transition widths Γ_0 are quoted, together with the reduced excitation probabilities $B(E1)\uparrow$ or $B(M1)\uparrow$. In cases of unknown parities, both excitation probabilities are given. In Tables V and VI, for the sake of completeness, the results of our former experiments on ^{112}Cd [43] and ^{114}Cd [44] without polarization measurements are included and are completed by the new polarization data.

IV. DISCUSSION

A. Systematics of dipole strength distributions

In Fig. 4 the dipole strength distributions in the investigated stable Cd isotopes are summarized. Plotted are the quantities $g\Gamma_0^{\rm red}$ [which are proportional to the reduced transition probabilities $B(E1)\uparrow$ or $B(M1)\uparrow$, see Eqs. (3) and (4)] as a function of the excitation energy. For the stronger excitations in the even-even isotopes, spins and parities have been determined from the angular distribution and linear polarization measurements. These assignments are given in the figure. The strongest $E1$ and $M1$ excitations are ascribed to $E1$ two-phonon excitations of the type $2^+\otimes 3^-$ and to excitations of 1^+ mixed-symmetry states, respectively. The systematics in the Cd isotopes of these general dipole modes are discussed in the following subsections.

Unfortunately, as discussed earlier, no spin and parity assignments were possible for the odd-mass isotopes ^{111,113}Cd. However, because of the low momentum transfer of real photons, the excitations predominantly should be of dipole character and should correspond to $E1$ and $M1$ transitions from the $1/2^+$ ground states to excited states with spins 1/2 or 3/2 of both parities. Looking at Fig. 4, it is obvious that the dipole strength distributions in the even-even isotopes can roughly be divided into two parts. The first part ranges from about 2200 to 3400 keV, and the second corresponds to the energy interval 3400 to 4100 keV. In the first group the transition strength is concentrated in a few strong transitions. All candidates for the $E1$ two-phonon excitations lie in this energy range. Conversely, in the second part the strength distributions differ for the various isotopes. For the lightest isotope ^{108}Cd, the strength is concentrated in only a few transitions. Going to the heavier isotopes the strength is more fragmented. For ^{110}Cd all transitions in the high-energy range are of $M1$ character. Unfortunately, for the heavier isotopes the parities of the weaker transitions in this energy range could not be measured. Assuming, nevertheless, $M1$ character for all transitions, the experimental findings can be interpreted as fragmentation of the $M1$ mode in this energy range.

In the odd-mass nuclei the dipole strengths, in addition to the strong excitation in ^{113}Cd at 2588 keV, are fragmented as compared to those in the neighboring even-even Cd isotopes. Furthermore, the observed total strengths are considerably reduced. A more quantitative discussion is presented in Sec. IV D.

B. $M1$ excitations to 1^+ mixed-symmetry states

Some strong observed $M1$ excitations in the even-even Cd-isotopes are interpreted as transitions to 1^+ mixed-symmetry states. As can be seen in the upper part of Fig. 5, their excitation energies vary smoothly from about 3.45 MeV in ^{108}Cd [42] to about 2.7 MeV in ^{116}Cd. For ^{108}Cd A. Gade *et al.* [42] compared experimental data taken with various spectroscopic methods with IBM-2 calculations and proposed the 3454-keV level as the lowest mixed-symmetry state. In ^{116}Cd the $M1$ strength seems to be fragmented into three states; therefore, an averaged excitation energy is plotted in Fig. 5. For the case of ^{112}Cd detailed IBM-2 calculations [14,19,43] support the interpretation of the 2931-keV level as a 1^+ mixed-symmetry state. Also for ^{108} Cd a recent IBM-2 calculation [42] supports the 3454-keV state as the lowest mixed-symmetry 1^+ state. The energies of the assigned 1^+ states in the Cd isotopes fit well into and extend the general systematics [46,47].

In the lower part of Fig. 5 the observed total $B(M1)\uparrow$ values are summarized (added up to 3.4 MeV). The full lines represent values expected in the U(5) (spherical vibrator) and O(6) (γ-soft rotor) limits [52]. The experimental data lie near to the U(5) values [$B(M1)\uparrow = 0$], whereas the O(6) values (using bare boson g factors) overestimate the experimental values by roughly a factor of 4. This is not surprising, because the even-even Cd nuclei are considered as among the best candidates for spherical vibrators. However, it should be noted that for ^{108}Cd, where detailed spectroscopic information is available [42], the decay pattern of the 3454-keV 1^+ mixed-symmetry state meets the expectations for a transitional nucleus on the path from U(5) to O(6) dynamical symmetry [42].

TABLE III. Results for dipole excitations in ^{111}Cd. Excitation energies E_x, total elastic-scattering cross sections $I_{S,0}$, the product of the statistical factor g times the ground-state widths Γ_0, the reduced ground-state widths $\Gamma_0^{\rm red}$, the decay branching ratios $R_{\rm expt}$[a], and the reduced excitation strengths, $B(M1)\uparrow$ and/or $B(E1)\uparrow$, are given.

E_x [keV]	$I_{S,0}$ [eV b]	$g\Gamma_0$ [meV]	$R_{\rm expt}$	$g\Gamma_0^{\rm red}$ [meV/MeV^3]	$B(M1)\uparrow$ [μ_N^2]	$B(E1)\uparrow$ [10^{-3}e^{2}fm^2]
2197	3.7(4)	4.59(22)	—	0.433(20)	0.037(4)	0.41(5)
2236	1.6(2)	2.14(8)	—	0.191(7)	0.017(3)	0.18(3)
2311	3.0(3)	4.16(9)	—	0.337(7)	0.029(3)	0.32(3)
2384	0.4(1)	0.60(2)	—	0.044(1)	0.004(1)	0.04(1)
2415[b]	1.9(8)	2.86(93)	1.93(61)	0.203(66)	0.018(6)	0.19(6)
2419	6.2(5)	9.38(33)	—	0.662(23)	0.057(4)	0.63(5)
2449	0.5(1)	0.83(2)	—	0.056(2)	0.005(1)	0.05(1)
2538	0.9(1)	1.57(3)	—	0.096(2)	0.008(1)	0.09(1)
2560	2.8(2)	4.72(7)	—	0.282(4)	0.024(2)	0.27(2)
2659	0.7(1)	1.37(3)	—	0.073(2)	0.006(1)	0.07(1)
2671	2.1(2)	3.94(6)	—	0.207(3)	0.018(2)	0.20(2)
2690	0.9(1)	1.70(3)	—	0.087(2)	0.008(1)	0.08(1)
2698[b]	0.9(1)	1.74(3)	—	0.089(2)	0.008(1)	0.08(1)
2708	1.8(2)	3.43(5)	—	0.173(3)	0.015(1)	0.16(1)
2730	0.9(1)	1.71(3)	—	0.084(2)	0.007(1)	0.08(1)
2756	0.7(1)	1.48(3)	—	0.071(1)	0.006(1)	0.07(1)
2775	1.5(1)	3.00(4)	—	0.141(2)	0.012(1)	0.13(1)
2788[b]	0.4(1)	0.82(3)	—	0.038(1)	0.003(1)	0.04(1)
2831[b]	0.6(1)	1.27(3)	—	0.056(1)	0.005(1)	0.05(1)
2858	2.9(2)	6.21(8)	—	0.266(3)	0.023(2)	0.25(2)
3039	2.4(1)	5.81(5)	—	0.207(2)	0.018(1)	0.20(1)
3059	1.2(6)	3.01(76)	1.71(72)	0.105(26)	0.009(3)	0.10(3)
3113	0.5(1)	1.29(2)	—	0.043(1)	0.004(1)	0.04(1)
3131	4.4(6)	11.21(103)	0.39(5)	0.365(34)	0.032(2)	0.35(2)
3147	0.7(1)	1.77(2)	—	0.057(1)	0.005(1)	0.05(1)
3173	1.9(1)	4.90(4)	—	0.153(1)	0.013(1)	0.15(1)
3185	0.8(1)	2.11(3)	—	0.065(1)	0.006(1)	0.06(1)
3207	1.1(2)	2.84(10)	—	0.086(3)	0.007(1)	0.08(1)
3246	0.8(1)	2.15(3)	—	0.063(1)	0.005(1)	0.06(1)
3259	0.7(1)	1.96(3)	—	0.057(1)	0.005(1)	0.05(1)
3302	1.8(2)	5.11(7)	—	0.142(2)	0.012(1)	0.14(1)
3323	1.3(3)	3.61(29)	0.78(2)	0.098(8)	0.009(1)	0.09(1)
3351	1.7(13)	4.92(457)	3.07(22)	0.131(121)	0.011(6)	0.12(7)
3362	1.1(1)	3.18(3)	—	0.084(1)	0.007(1)	0.08(1)
3384	0.9(1)	2.64(3)	—	0.068(1)	0.006(1)	0.07(1)
3394	0.8(1)	2.31(3)	—	0.059(1)	0.005(1)	0.06(1)
3455	2.6(2)	8.18(16)	—	0.198(4)	0.017(1)	0.19(2)
3467	6.7(8)	20.81(187)	0.27(3)	0.500(45)	0.043(2)	0.48(2)
3483	3.5(5)	10.95(80)	0.67(9)	0.259(19)	0.022(2)	0.25(2)
3498	2.7(2)	8.53(8)	—	0.199(2)	0.017(1)	0.19(1)
3526	8.7(9)	28.15(249)	4.69(34)	0.642(57)	0.055(5)	0.61(6)
3542	1.6(1)	5.33(5)	—	0.120(1)	0.010(1)	0.11(1)
3553	0.7(1)	2.34(4)	—	0.052(1)	0.005(1)	0.05(1)
3566	0.8(1)	2.75(4)	—	0.061(1)	0.005(1)	0.06(1)
3573	0.7(1)	2.19(4)	—	0.048(1)	0.004(1)	0.05(1)
3671	0.4(1)	1.27(4)	—	0.026(1)	0.002(1)	0.02(1)
3691	0.6(1)	2.26(5)	—	0.045(1)	0.004(1)	0.04(1)
3702	1.5(2)	5.23(8)	—	0.103(2)	0.009(1)	0.10(1)
3710	2.3(2)	8.09(13)	—	0.158(3)	0.014(1)	0.15(1)
3715	0.6(1)	2.12(7)	—	0.041(1)	0.004(1)	0.04(1)
3733	0.4(1)	1.58(7)	—	0.030(1)	0.003(1)	0.03(1)
3740	2.6(2)	9.59(18)	—	0.183(3)	0.016(1)	0.18(1)
3756	0.6(1)	2.27(8)	—	0.043(2)	0.004(1)	0.04(1)
3781	0.5(1)	2.03(7)	—	0.038(1)	0.003(1)	0.04(1)
3801	0.9(2)	3.31(10)	—	0.060(2)	0.005(1)	0.06(1)

TABLE III. *(Continued.)*

E_x [keV]	$I_{S,0}$ [eV b]	$g\Gamma_0$ [meV]	R_{expt}	$g\Gamma_0^{\text{red}}$ [meV/MeV^3]	$B(M1)\uparrow$ [μ_N^2]	$B(E1)\uparrow$ [10^{-3}e^{2}fm^2]
3828	3.5(7)	13.24(164)	1.66(25)	0.236(29)	0.020(3)	0.23(3)
3856	4.7(13)	18.33(613)	0.76(15) 1.33(20)[c]	0.320(107)	0.028(3)	0.31(4)
3900	2.8(2)	10.91(20)	—	0.184(3)	0.016(1)	0.18(1)
3921	0.8(2)	3.11(18)	—	0.052(3)	0.004(1)	0.05(1)

[a]The quoted decay branching ratios correspond to those to first excited $5/2^+$ state at 245 keV.
[b]Possibly a transition to the second excited state ($3/2^+$) at 342 keV.
[c]Decay branching ratio to the second excited state ($3/2^+$) at 342 keV.

TABLE IV. Results for the reaction ^{110}Cd$(\gamma, \vec{\gamma}')$. The measured excitation energies E_x, the integrated scattering cross sections $I_{S,0}$, branching ratios R_{expt}[a] for the decay to the first excited 2^+ state at 658 keV, and azimuthal asymmetries ε are summarized. Ground-state transition widths Γ_0, assigned spins and parities J^π, and reduced transition probabilities $B(M1)\uparrow$ and $B(E1)\uparrow$ were deduced.

E_x [keV]	$I_{S,0}$ [eV b]	R_{expt}	ϵ [%]	J^π	Γ_0 [meV]	$B(M1)\uparrow$ [μ_N^2]	$B(E1)\uparrow$ [10^{-3}e^{2}fm^2]
2650	25.1(6)	—	−11(5)	1^-	15.3(4)	—	2.35(5)
3044	21.8(30)	0.38(5)	6(5)	1^+	17.6(6)	0.161(5)	—
3079	9.5(17)	4.53(65)	—	1	7.8(12)	0.069(10)	0.77(11)
3281	13.1(4)	—	3(6)	$1^{(+)}$	12.2(4)	0.090(3)	0.99(3)
3298	3.6(3)	—	—	1	3.4(3)	0.025(2)	0.27(2)
3359	40.0(8)	—	−14(4)	1^-	39.1(8)	—	2.96(6)
3475	6.0(3)	—	—	1	6.3(3)	0.039(2)	0.43(2)
3598	5.7(4)	—	24(16)	1^+	6.4(5)	0.036(3)	—
3772	37.7(40)	0.54(5)	13(8)	1^+	46.5(17)	0.225(8)	—
3854	7.7(10)	—	9(7)[b]	$1^{(+)}$	9.9(13)	0.045(6)	0.50(6)
3862	29.7(98)	0.21(7)	9(7)[b]	$1^{(+)}$	38.4(21)	0.173(10)	1.91(11)

[a]Decay branchings have been observed only to the first excited 2^+ state at 658 keV.
[b]The transitions at 3854 and 3862 keV could not be resolved in the polarization measurements. The quoted large positive asymmetry corresponds to the asymmetry of the unresolved doublet.

TABLE V. Results for the reaction ^{112}Cd$(\gamma, \vec{\gamma}')$ together with those from our previous ^{112}Cd(γ, γ') work [43]. The listed quantities are the same as in Table IV.

E_x [keV]	$I_{S,0}$ [eV b]	R_{expt}[a]	ε [%]	J^π	Γ_0 [meV]	$B(M1)\uparrow$ [μ_N^2]	$B(E1)\uparrow$ [10^{-3} e^{2}fm^2]
2418	0.7(1)	—		$(1,2^+)$	0.34(7)	0.006(1)	0.07(1)
2506	16.7(8)	—	−10(8)	1^-	9.1(4)		1.65(8)
2694	1.0(2)	—		1	0.7(1)	0.009(1)	0.10(1)
2829	4.5(3)	—		1	3.1(2)	0.035(2)	0.39(2)
2931	12.4(6)	0.89(7)	8(10)	$1^{(+)}$	13.3(5)	0.137(5)	1.52(6)
3133	26.1(11)	—	−13(6)	1^-	22.2(10)		2.07(9)
3231	9.8(5)	—	27(12)	1^+	8.8(4)	0.068(3)	
3300	7.5(4)	0.67(9)		1	9.6(5)	0.069(4)	0.77(4)
3375	1.4(2)	—		$(1,2^+)$	1.4(2)	0.009(1)	0.10(1)
3557	0.8(2)	—		$(1,2^+)$	0.9(2)	0.005(1)	0.06(2)
3568	0.9(2)	—		(1)	1.0(2)	0.006(1)	0.07(1)
3594	1.3(2)	—		1	1.4(2)	0.008(1)	0.09(2)
3683	4.4(7)	—		1	5.1(8)	0.027(4)	0.29(4)
3704	5.9(5)	—		1	7.0(5)	0.036(3)	0.40(3)
3810	17.3(11)	0.19(3)		1	24.2(15)	0.11(1)	1.26(8)
3846	1.8(3)	—		1	2.4(4)	0.011(2)	0.12(2)
3869	11.3(9)	0.42(8)		1	18.3(13)	0.082(6)	0.90(6)
3933	4.5(6)	—		1	6.1(8)	0.026(4)	0.29(4)
3997	6.3(10)	—		$(1,2^+)$	8.7(14)	0.035(6)	0.39(6)

[a]Decay branchings have been observed only to the first excited 2^+ state at 617 keV. The decay branchings quoted have been calculated from the original data of Ref. [43].

TABLE VI. Results for the reaction ^{114}Cd($\gamma, \vec{\gamma}'$), together with those from our previous ^{114}Cd(γ, γ') work [44]. The listed quantities are the same as in Table IV.

E_x [keV]	$I_{S,0}$ [eV b]	R_{expt}[a]	ϵ [%]	J^π	Γ_0 [meV]	$B(M1)\uparrow$ [μ_N^2]	$B(E1)\uparrow$ [$10^{-3}e^2\text{fm}^2$]
2396	1.4(4)	—	−11(7)	1^-	0.7(2)	—	0.14(4)
2456	20.9(35)	—	−12(2)	1^-	11.0(18)	—	2.12(36)
2646	1.0(3)	—	—	1	0.6(2)	0.008(2)	0.09(3)
2650	1.2(4)	—	—	1	0.8(2)	0.010(3)	0.12(4)
2768	10.9(13)	—	−14(6)	1^-	7.2(8)	—	0.97(11)
2800	16.6(25)	0.43(4)	7(4)	1	11.3(13)	0.134(15)	—
3000	14.2(27)	0.42(7)	—	1	11.1(11)	0.107(10)	1.18(11)
3110	20.5(19)	0.92(5)	1(4)[b]	$1^{(+)}$	17.2(13)	0.148(12)	1.64(13)
3214	2.7(3)	—	16(4)[c]	$1^{(+)}$	2.5(3)	0.019(2)	0.21(3)
3220	14.0(9)	—	16(4)[c]	$1^{(+)}$	12.6(8)	0.098(6)	1.08(7)
3748	9.7(14)	0.61(8)	—	1	11.9(9)	0.058(4)	0.65(5)
3791	1.1(4)	—	—	1	1.4(5)	0.007(2)	0.07(2)
3796	2.5(7)	—	—	1	3.1(9)	0.015(4)	0.16(5)
3827	3.6(17)	2.7(11)	—	1	4.5(14)	0.021(6)	0.23(7)
3857	2.5(5)	—	—	1	3.2(6)	0.014(3)	0.16(3)
3916	5.9(12)	—	—	1	7.8(16)	0.034(7)	0.37(8)
3949	4.6(11)	—	—	1	6.2(15)	0.026(6)	0.29(7)
3994	9.1(19)	—	—	1	12.6(26)	0.051(11)	0.57(12)

[a]Decay branchings have been observed only to the first excited 2^+ state at 538 keV.
[b]In our previous high-resolution measurement [44], transitions at 3109 and 3110 keV were observed but could not be resolved in the present polarization measurements.
[c]The transitions at 3214 and 3220 keV could not be resolved in the present polarization measurements.

TABLE VII. Results for the reaction ^{116}Cd($\gamma, \vec{\gamma}'$). The listed quantities are the same as in Table IV.

E_x [keV]	$I_{S,0}$ [eV b]	R_{expt}[a]	ϵ [%]	Spin J^π	Γ_0 [meV]	$B(M1)\uparrow$ [μ_N^2]	$B(E1)\uparrow$ [$10^{-3}\text{e}^2\text{fm}^2$]
2478	18.2(11)	—	−7(4)	1^-	9.7(6)	—	1.82(11)
2488[b]	3.9(6)	—	3(6)	1^+	2.1(3)	0.035(6)	—
2659	7.3(7)	—	11(7)	1^+	4.5(4)	0.062(6)	—
2762	3.0(7)	—	—	1	2.0(5)	0.025(6)	0.27(6)
2829	20.8(27)	0.72(8)	−5(3)	1^-	14.5(10)	—	1.83(13)
2845	9.8(23)	3.53(67)	29(13)	1^+	6.9(13)	0.077(15)	—
3068	25.4(12)	—	4(3)	1^+	20.7(10)	0.186(9)	—
3156	6.0(6)	—	−10(7)	1^-	5.2(5)	—	0.48(5)
3282	1.0(6)	—	—	1	0.9(6)	0.007(4)	0.08(5)
3401	1.7(4)	—	—	1	1.7(4)	0.011(3)	0.13(3)
3423	2.8(5)	—	11(27)	1^+	2.8(5)	0.018(3)	—
3601	5.7(5)	—	—	1	6.4(6)	0.036(3)	0.39(4)
3641	1.1(3)	—	—	1	1.3(4)	0.007(2)	0.08(2)
3655	3.6(21)	0.76(43)	—	1	4.2(10)	0.022(5)	0.25(6)
3732	5.5(5)	—	—	1	6.7(7)	0.033(3)	0.37(4)
3763	1.9(6)	—	—	1	2.4(7)	0.012(4)	0.13(4)
3782	8.1(29)	0.67(23)	—	1	10.0(14)	0.048(7)	0.53(7)
3849	6.7(6)	—	—	1	8.6(8)	0.039(4)	0.43(4)
3876	4.3(5)	—	—	1	5.6(7)	0.025(3)	0.27(3)
3895	14.1(38)	0.74(19)	—	1	18.6(21)	0.082(9)	0.90(10)
3976	3.2(5)	—	—	1	4.4(7)	0.018(3)	0.20(3)
3997	1.6(5)	—	—	1	2.2(7)	0.009(3)	0.10(3)
4027	4.7(6)	—	—	1	6.7(9)	0.027(4)	0.29(4)

[a]Decay branchings have been observed only to the first excited 2^+ state at 513 keV.
[b]Eventually $E2$ transition with $\Gamma_0 = 2.1(3)$ meV and $B(E2)\uparrow = 137(20)$ e^2fm^4.

TABLE VIII. $E1$ two-phonon excitations in the even-A Cd isotopes ($Z = 48$). Given are the experimentally observed excitation energies E_{1^-} of the 1^- levels of the two-phonon quintuplet ($2^+ \otimes 3^-$) together with the energies of the corresponding one phonon excitations E_{2^+} and E_{3^-} and their sums ($E_{2^+} + E_{3^-}$) . In addition, excitation strengths $B(E1) \uparrow$ are reported.

Isotope	E_{1^-} [keV]	E_{2^+} [keV]	E_{3^-} [keV]	$(E_{2^+} + E_{3^-})$ [keV]	$B(E1) \uparrow$ [10^{-3} e^{2}fm^2]	Ref.
^{108}Cd	2678	633	2202	2835	2.49(10)	[42]
^{110}Cd	2650	658	2079	2735	2.35(5)	This work
^{112}Cd	2506	618	2005	2623	1.66(8)[a]	[43]
^{114}Cd	2456	558	1958	2516	2.12(36)	This work
^{116}Cd	2478	513	1922	2435	1.82(11)	This work

[a]Assuming $\Gamma_0/\Gamma = 1$, the decay branching reported in Ref. [19] could not be confirmed in the photon-scattering experiments [43].

C. *E*1 two-phonon excitations

1. E1 two-phonon excitations in the Cd isotopes

The data show the existence of dipole excitations of $E1$ and $M1$ character. In the even-A Cd isotopes, for which parity assignments were possible, two similary strong $E1$ excitations were observed with an energy difference of 300–700 keV. Because of the close match of the excitation energy of the lower lying of these two 1^- states the lower lying 1^- state is considered as the $2^+ \otimes 3^-$ quadrupole-octupole coupled 1^- state.

Figure 6 summarizes the experimental findings observed for the even-even Cd isotopes. The excitation energies of the $E1$ two-phonon excitations are shown in the upper part of the figure as full circles. They lie quite close at the sum energy $\Sigma = E_{2^+} + E_{3^-}$ of the corresponding quadrupole and octupole single-phonon excitations. This documents a rather harmonic coupling. In the lower part of the figure, the observed reduced excitation probabilities $B(E1) \uparrow$ are depicted. The strengths decrease smoothly with the increasing mass numbers A of the isotopes (see Table VIII).

2. Systematics of E1 two-phonon excitations in nuclei near the Z = 50 shell closure and an explanation within a macroscopic model

Figure 7 shows the reduced transition probabilities $B(E1, 1^- \rightarrow 0^+) = \frac{1}{3}\, B(E1, 0^+ \rightarrow 1^-)$ for the low-lying $E1$ ground-state transitions of the 1^- two-phonon states in even-even nuclei near the $Z = 50$ shell closure, which is emphasized by the bold line. Clearly, the $B(E1) \downarrow$ values are greatest for the Sn isotopes ($Z = 50$) [36]. The strengths observed

TABLE IX. Integrated dipole strengths observed in photon scattering experiments with the isotopes ^{108,110,111,112,113,114,116}Cd in the energy intervals 3.4–4.0 and 1.0–4.0 MeV, respectively. A value of $g\Gamma_0^{\rm red} = 1$ meV/MeV^3 corresponds to excitation strengths of $B(E1) \uparrow = 0.955\ 10^{-3}$ e^2 fm^2 or $B(M1) \uparrow = 0.0864\ \mu_N^2$, see Eqs. (3) and (4).

Isotope	$\sum_{3.4\rm MeV}^{4.0\rm MeV} g\Gamma_0^{\rm red}$ [meV/MeV^3]	$\sum_{1.0\rm MeV}^{4.0\rm MeV} g\Gamma_0^{\rm red}$ [meV/MeV^3]	Ref.
^{108}Cd	3.55(12)	11.69(22)	[42]
^{110}Cd	5.98(14)	15.54(22)	This work
^{111}Cd	3.58(16)	9.07(27)	This work
^{112}Cd	4.03(15)	11.80(21)	[43]
^{113}Cd	2.43(19)	8.54(28)	[44]
^{114}Cd	2.70(20)	8.54(28)	This work
	3.80(26)	12.61(49)	[44]
^{116}Cd	4.35(19)	13.22(35)	This work

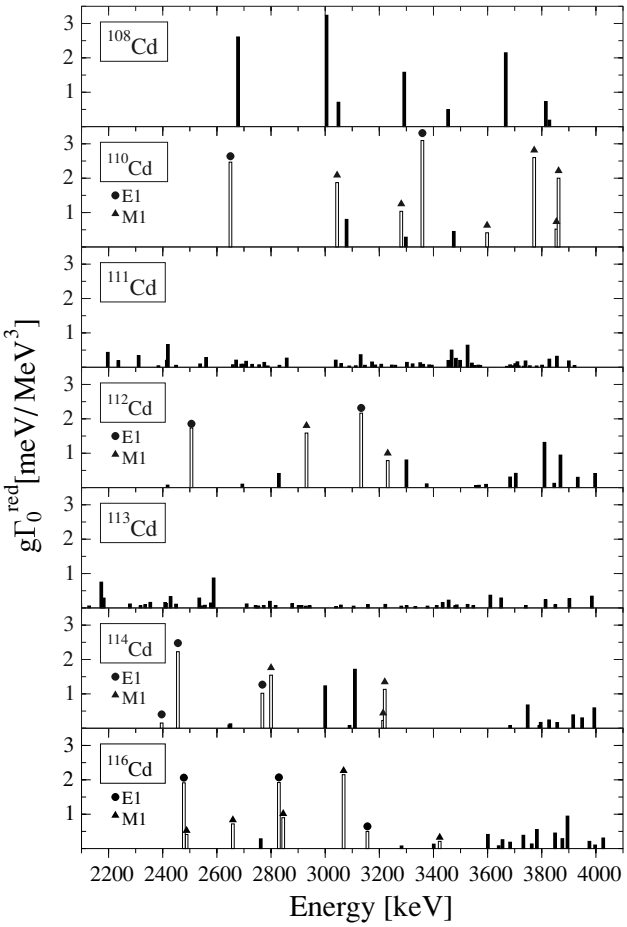

FIG. 4. Systematics of dipole strength distributions in ^{108,110,111,112,113,114,116}Cd observed in NRF experiments. Plotted is the quantity $g\Gamma_0^{\rm red}$ as a function of the excitation energy. A value of $g\Gamma_0^{\rm red} = 1$ meV/MeV^3 corresponds to excitation strengths of $B(E1) \uparrow = 0.95510^{-3}$ e^2 fm^2 or $B(M1) \uparrow = 0.0864\ \mu_N^2$ [see Eqs. (3) and (4)]. Assigned spins and parities of states in the even-even nuclei are marked, their strengths are shown by open bars. The strengths for dipole excitations of unknown parities are depicted by full bars. The excitations in the odd mass isotopes are most probably of dipole character (see text).

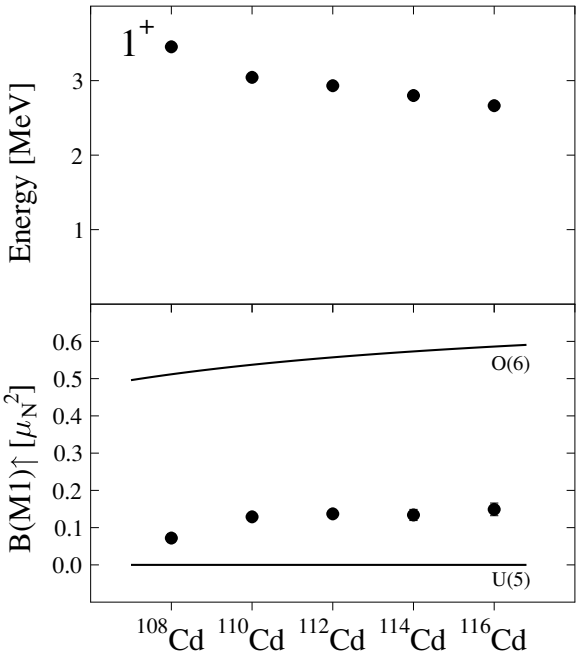

FIG. 5. Excitation energies and strengths $B(M1\uparrow)$ of low-lying mixed-symmetry 1^+ states in the stable even-even Cd isotopes ^{108,110,112,114,116}Cd observed in the Stuttgart NRF experiments.

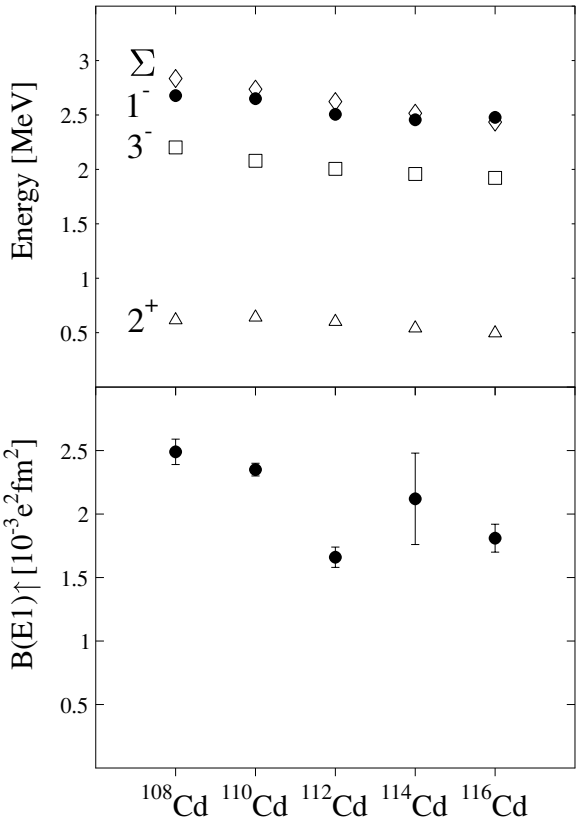

FIG. 6. Systematics of $E1$ two-phonon excitations in the even-even Cd isotopes. (Upper) Energies of the 2_1^+ (open triangles) and 3_1^- (open squares) one-phonon excitations and of the observed 1^- two-phonon excitations (full circles) in ^{108,110,112,114,116}Cd compared to the expected sum energies $\Sigma = E_{2^+} + E_{3^-}$ (open rhombs). (Lower) Experimental $B(E1)\uparrow$ values for the two-phonon excitations. Error bars are smaller than the symbol size if not explicitely depicted.

in the present experiments for the Cd isotopes ($Z = 48$) and Te isotopes ($Z = 52$) [53,54], with two protons below and above the $Z = 50$ closed shell, are about a factor of 3 lower than those for the Sn isotopes. Such behavior was generally found for shell closures [35] and could be explained by the dipole core polarization effect [35] and also in the framework of the microscopic quasiparticle-phonon model (QPM) [55]. Another successful description of the enhanced electric dipole transitions in nuclei near shell closures with strong collective correlations was provided by Jolos and Scheid [56] in the framework of a model based on cluster-type correlations. Also, the Q-phonon scheme provided a satisfactory description of the properties of low-lying 1^- states in spherical nuclei and their decay characteristics [57].

Here we present an intuitive explanation of the different strengths of the two-phonon excitations in the magic Sn isotopes and the neighboring Cd and Te isotopes in terms of a macroscopic vibration of valence nucleons against a closed core.

The transition strengths of dipole excitations are proportional to the squares of the electric dipole moments. Bohr and Mottelson [58] and also Strutinski [59] deduced the following expression for the corresponding electric dipole moment D_{BM} for nuclei with quadrupole and octupole deformations:

$$D_{\mathrm{BM}} = 5.367\ 10^{-4}(Z+N)Z\ \beta_2\ \beta_3\ [\mathrm{e\ fm}]. \tag{8}$$

The deformation parameters β_2 and β_3 can be determined from the quadrupole and octupole reduced transition probabilities $B(E2, 0_1^+ \rightarrow 2_1^+)$ and $B(E3, 0_1^+ \rightarrow 3_1^-)$, respectively. Numerical values are available in the compilations of Refs. [60] and [61].

In Fig. 8 the observed $E1$ excitation strengths $B(E1)\uparrow$ divided by the squared dipole moments D_{BM} are plotted. Obviously, the values for the Cd isotopes ($Z = 48$) and Te isotopes ($Z = 52$) are nearly constant and agree with the expectation of a general proportionality between the $B(E1)\uparrow$ values and D_{BM}^2. The scaling constant is in agreement with the factor found by Babilon *et al.* [62–64] in an extended systematics for numerous nuclei away from closed shells. Conversely, the ratios $B(E1)\uparrow / D_{\mathrm{BM}}^2$ for the magic Sn nuclei ($Z = 50$) are much higher and, furthermore, increase linearly with neutron number. To explain these experimental findings, which clearly hint at a shell effect, the nucleons are divided within a simple macroscopic model into core and valence nucleons. Denoting the center-of-mass coordinate of the core nucleons R_c and that of the valence nucleons $R_v = R_c + \Delta$, the corresponding center of mass coordinates R_p and R_n for the protons and neutrons are as follows:

$$R_p = \frac{Z_c}{Z} R_c + \frac{Z_v}{Z}(R_c + \Delta) \tag{9}$$

$$R_n = \frac{N_c}{N} R_c + \frac{N_v}{N}(R_c + \Delta), \tag{10}$$

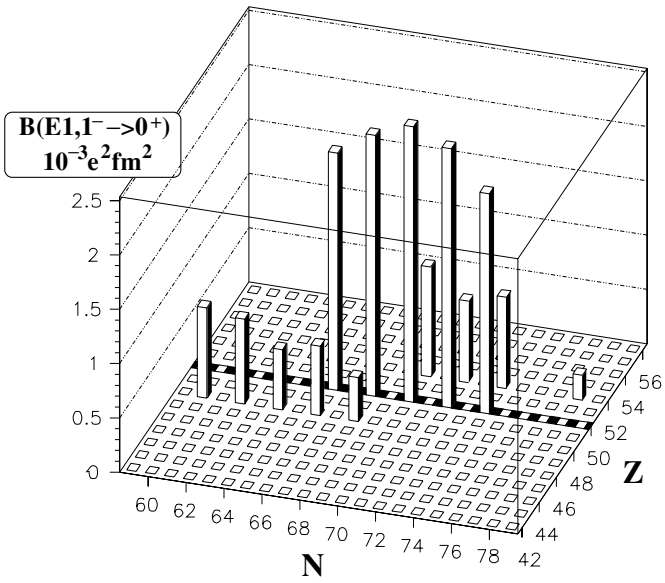

FIG. 7. Reduced transition probabilities $B(E1, 1^- \to 0^+) = \frac{1}{3}B(E1, 0^+ \to 1^-)$ for $E1$ ground-state transitions from the two-phonon 1^- states in spherical nuclei near the $Z = 50$ shell closure. Data are from the recent compilation of Ref. [35] have been supplemented with the new Cd data.

where Z_c, Z_v and N_c, N_v are the numbers of core and valence protons and neutrons, respectively. These expressions can be inserted into the general relation for the electric dipole moment D

$$D = e\,\frac{NZ}{A}\,(R_p - R_n), \tag{11}$$

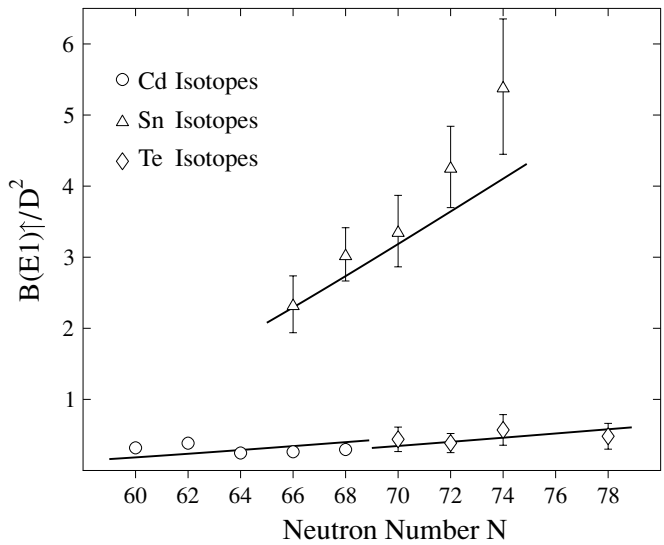

FIG. 8. Ratios of the $E1$ excitation strengths $B(E1; 0^+ \to 1^-)$ and the squares of the electric dipole moments $D^2_{\rm BM}$ for the even-A Cd, Sn [36], and Te [53,54] isotopes. The full lines represent the calculations described in the text.

resulting in an effective dipole moment $D_{\rm eff}$

$$D_{\rm eff} = e\,\frac{NZ}{A}\left(\frac{N_c}{N} - \frac{Z_c}{Z}\right)\Delta, \tag{12}$$

which depends on Z, N, and A, as well as the parameters Z_c, N_c, and Δ. An equivalent relation was derived by Iachello [65] within a cluster model. By an adequate choice of the numbers of core nucleons, Z_c and N_c, the shell structure now can be explicitly taken into account. Conversely, a collective dipole motion, ignoring shell structures, possesses a nonvanishing dipole moment $D_{\rm coll}$ as follows:

$$D_{\rm coll} = e\left(\frac{NZ}{A}\right)\Delta. \tag{13}$$

To connect the effective and the collective dipole moments the following ansatz is used:

$$D_{\rm eff} = K(N)D_{\rm coll}, \tag{14}$$

where $K(N)$ can be interpreted as a correction factor taking into account the shell effects. From this ansatz and Eqs. (12) and (13) one obtains the following:

$$K(N) = \frac{N_c}{N} - \frac{Z_c}{Z}. \tag{15}$$

The lines in Fig. 8 are given by the products of the square of $K(N)$ and a scaling factor s_Z. This factor ensures that the first moment of the $B(E1, 0^+_{\rm GS} \to 1^-_1)/D^2_{\rm BM}$ values equals the average of the respective $s_Z K(N)^2$ values within each isotopic chain.

The Cd and Te isotopes are described by a core of $Z_C = 28$ protons and $N_C = 28$ neutrons, whereas the Sn isotopes are ascribed a core of 50 protons and 50 neutrons. As can shown in Fig. 8, the calculations (full lines) describe the experimental data quite well. This result might seem to be surprising, however, it should be emphasized, that alternative choices of the cores lead to clear discrepancies between the calculated values and the experimental findings [66]. In particular, choosing a core of 28 neutrons and protons for the Sn isotopes, as for the Cd and Te isotopes, and assuming a scaling of the dipole strengths with the effective dipole moment $D_{\rm eff}$, the strengths calculated for the Sn isotopes fit well into the systematics of the experimental data for the Cd and Te isotopes [66]. This can be interpreted as a further evidence for a $N_c = Z_c = 28$ core in the Cd and Te isotopes. Conversely, one would expect from the shell model that the core for the Cd isotopes should consists of 50 neutrons and 28 protons and that of the Te nuclei of 50 neutrons and protons. Obviously, this is not the case. Nucleons from inner shells seem to play an important role in the dipole excitations. This observation can be interpreted as a dipole core polarization effect, which has already been described in a collective picture [67] and by microscopic calculations [68].

Further support for the macroscopic description is provided by the explanation of the observed excitation energies of the two-phonon excitations. These energies are systematically higher in the Sn isotopes (3.3–3.5 MeV) [36] than in the Cd and Te isotopes [53,54] (2.3–2.8 MeV). This difference can be explained within a simple harmonic oscillator picture. Here

the oscillation frequency ω is given by the following:

$$\omega = \sqrt{\frac{k}{m_r}}, \tag{16}$$

where k and m_r are the oscillator restoring force and the reduced mass, respectively. The reduced mass depends on the division into valence and core nucleons. Under the assumption that the energies for different cores scale according Eq. (16) the excitation energies in the Sn isotopes for a hypothetical $N_c, Z_c = 28$ core can be calculated. The results are shifted down from the experimental data and agree quite well with the energies observed experimentally in the Te and Cd isotopes [66].

D. Fragmentation of the dipole strengths in the odd-mass Cd isotopes

In Table IX the total integrated dipole strengths observed in the Cd isotopes are summarized. Values are given for two integration intervals, the entire investigated energy range from 1 to 4 MeV and the high-energy interval 3.4–4 MeV. For ^{114}Cd the results of the present polarization sensitive measurements and those from our previous high-resolution study [44] are given. The slight differences of the two data sets at higher energies can be explained by the different sensitivities in the experiments.

From the assumption that the strengths in the high-energy part are of $M1$ character, one would expect a roughly constant total strength in this energy range, in fair agreement with the observation. On the other hand, the total strengths in the complete energy range up to 4 MeV observed in the odd-mass isotopes ^{111,113}Cd is reduced by about 25–40%, as compared to those in the neighboring even-even isotopes. This discrepancy can be explained by the strong fragmentation of the strengths because of the various possible couplings of the odd particle or hole to the core excitation modes. A nonnegligible fraction of these excitations have strengths that are too low to be detected in the photon-scattering experiments. The same effect was observed in the odd-mass Sn [69,70] and Sb [71] isotopes around $Z = 50$ and the odd-mass Ba isotopes [72] around $N = 82$. This explanation is supported by measurements with different sensitivities and a fluctuation analysis of the spectra in the case of the deformed nuclei ^{163}Dy and ^{165}Ho [73].

V. CONCLUSIONS

From the present photon-scattering experiments dipole strength distributions in the vibrational nuclei ^{108,110,111,112,113,114,116}Cd up to an excitation energy of 4 MeV were determined. For excitations in the even-A isotopes parities were assigned from linear polarization measurements. Systematics of $E1$ two-phonon excitations to the 1^- member of the $2^+ \otimes 3^-$ quintuplet and of $M1$ excitations to mixed-symmetry 1^+ states were established. The observed reduced strengths of the two-phonon excitations, compared to those in the neighboring magic Sn isotopes, is explained in a macroscopic picture in terms of a vibration of valence nucleons against a closed core. In both odd-mass isotopes ^{111,113}Cd an overall fragmentation of the dipole strengths was observed.

ACKNOWLEDGMENTS

The financial support of the Stuttgart projects by the Deutsche Forschungsgemeinschaft (DFG) under contracts Kn 154/30,31, Br799/11, and Jo391/3-1 is gratefully acknowledged. N.P. thanks the Department of Energy for his support under grant DE-FGO2-04ER41334. This material is based on work supported by the U.S. National Science Foundation under grant PHY-0354656.

[1] R. F. Casten, *Nuclear Structure from a Simple Perspective* (Oxford University Press, New York Oxford, 1990).
[2] A. Aprahamian, D. S. Brenner, R. F. Casten, R. L. Gill, A. Piotrowski, and K. Heyde, Phys. Lett. **B140**, 22 (1984).
[3] A. Aprahamian, D. S. Brenner, R. F. Casten, R. L. Gill, and A. Piotrowski, Phys. Rev. Lett. **59**, 535 (1987).
[4] M. Délèze, S. Drissi, J. Kern, P. A. Tercier, J. P. Vorlet, J. Rikovska, T. Otsuka, S. Judge, and A. Williams, Nucl. Phys. **A551**, 269 (1993).
[5] A. Gade, J. Jolie, and P. von Brentano, Phys. Rev. C **65**, 041305(R) (2002).
[6] A. Gade and P. von Brentano, Phys. Rev. C **66**, 014304 (2002).
[7] M. Kadi, N. Warr, P. E. Garret, J. Jolie, and S. W. Yates, Phys. Rev. C **68**, 031306(R) (2003).
[8] K. Heyde, P. Van Isacker, M. Waroquier, G. Wenes, and M. Sambataro, Phys. Rev. C **25**, 3160 (1982).
[9] J. Kern, A. Bruder, S. Drissi, V. A. Ionescu, and D. Kusnezov, Nucl. Phys. **A512**, 1 (1990).
[10] J. Jolie and H. Lehmann, Phys. Lett. **B342**, 19 (1995).
[11] H. Lehmann and J. Jolie, Nucl. Phys. **A588**, 19 (1995).
[12] P. H. Regan, C. W. Beausang, N. V. Zamfir, R. F. Casten, Jing-ye Zhang, A. D. Yamamota, M. A. Caprio, G. Gürdal, A. A. Hecht, C. Hutter, R. Krücken, S. D. Langdown, D. A. Meyer, and J. J. Ressler, Phys. Rev. Lett. **90**, 152502 (2003).
[13] R. F. Casten, J. Jolie, H. G. Börner, D. S. Brenner, N. V. Zamfir, W.-T. Chou, and A. Aprahamian, Phys. Lett. **B297**, 19 (1992).
[14] M. Délèze, S. Drissi, J. Jolie, J. Kern, and J. P. Vorlet, Nucl. Phys. **A554**, 1 (1993).
[15] F. Corminboeuf, T. B. Brown, L. Genilloud, C. D. Hannant, J. Jolie, J. Kern, N. Warr, and S. W. Yates, Phys. Rev. Lett. **84**, 4060 (2000).
[16] F. Corminboeuf, T. B. Brown, L. Genilloud, C. D. Hannant, J. Jolie, J. Kern, N. Warr, and S. W. Yates, Phys. Rev. C **63**, 014305 (2000).
[17] H. Lehmann, P. E. Garrett, J. Jolie, C. A. McGrath, M. Yeh, and S. W. Yates, Phys. Lett. **B387**, 259 (1996).

[18] D. Bandyopadhyay, C. C. Reynolds, S. R. Lesher, C. Fransen, N. Boukharouba, M. T. McEllistrem, and S. W. Yates, Phys. Rev. C **68**, 014324 (2003).
[19] S. E. Drissi, P. A. Tercier, H. G. Börner, M. Délèze, F. Hoyler, S. Judge, J. Kern, S. J. Mannanal, G. Mouze, K. Schreckenbach, J. P. Vorlet, N. Warr, A. Williams, and C. Ythier, Nucl. Phys. **A614**, 137 (1997).
[20] P. E. Garrett, H. Lehmann, J. Jolie, C. A. McGrath, M. Yeh, and S. W. Yates, Phys. Rev. C **59**, 2455 (1999).
[21] R. A. Gatenby, J. R. Vanhoy, E. M. Baum, E. L. Johnson, S. W. Yates, T. Belgya, B. Fazekas, Á. Veres, and G. Molnár, Phys. Rev. C **41**, R414 (1990).
[22] J. R. Vanhoy, J. M. Anthony, B. M. Haas, B. H. Benedict, B. T. Meehan, Sally F. Hicks, C. M. Davoren, and C. L. Lundstedt, Phys. Rev. C **52**, 2387 (1995).
[23] C. Fahlander, A. Bäcklin, L. Hasselgren, A. Kavka, V. Mittal, L. E. Svensson, B. Varnestig, D. Cline, B. Kotlinski, H. Grein, E. Grosse, R. Kulessa, C. Michel, W. Spreng, H. J. Wollersheim, and J. Stachel, Nucl. Phys. **A485**, 327 (1988).
[24] A. Mheemeed, K. Schreckenbach, G. Barreau, H. R. Faust, H. G. Börner, R. Brissot, F. Hungerford, H. H. Schmidt, H. J. Scheerer, T. von Egidy, K. Heyde, J. L. Wood, P. van Isacker, M. Waroquier, G. Wenes, and M. L. Stelts, Nucl. Phys. **A412**, 113 (1984).
[25] R. Hertenberger, G. Eckle, F. J. Eckle, G. Graw, D. Hofer, H. Kader, P. Schiemenz, Gh. Cata-Danil, C. Hategan, N. Fujiwara, K. Hosono, M. Kondo, M. Matsuoka, T. Noro, T. Saito, S. Kato, S. Matsuki, N. Blasi, S. Micheletti, and R. de Leo, Nucl. Phys. **A574**, 414 (1994).
[26] M. Bertschy, S. Drissi, P. E. Garrett, J. Jolie, J. Kern, S. J. Mannanal, J. P. Vorlet, N. Warr, and J. Suhonen, Phys. Rev. C **51**, 103 (1995).
[27] Youba Wang, P. Dendooven, J. Huikari, A. Jokinen, V. S. Kolhinen, G. Lhersonneau, A. Nieminen, S. Nummela, H. Penttilä, K. Peräjärvi, S. Rinta-Antila, J. Szerypo, J. C. Wang, and J. Äystö, Phys. Rev. C **64**, 054315 (2001).
[28] A. Gade, A. Fitzler, C. Fransen, J. Jolie, S. Kasemann, H. Klein, A. Linnemann, V. Werner, and P. von Brentano, Phys. Rev. C **66**, 034311 (2002).
[29] P. E. Garrett, H. Lehmann, J. Jolie, C. A. McGrath, Minfang Yeh, W. Younes, and S. W. Yates, Phys. Rev. C **64**, 024316 (2001).
[30] D. Bandyopadhyay, C. C. Reynolds, C. Fransen, N. Boukharouba, M. T. McEllistrem, and S. W. Yates, Phys. Rev. C **67**, 034319 (2003).
[31] J. Kern, Phys. Lett. **B320**, 7 (1994).
[32] Z. Németh, T. Belgya, B. Fazekas, G. Molnár, E. M. Baum, E. L. Johnson, D. P. DiPretre, D. Wang, S. W. Yates, D. Hofer, S. Faber, G. Graw, R. Kokowski, E. Müller-Zanotti, G. Cata-Danil, W. Geiger, I. Bauske, R. D. Heil, U. Kneissl, J. Margraf, H. H. Pitz, P. von Brentano, R.-D. Herzberg, A. Zilges, C. Wesselborg, N. Warr, M. Bertschy, M. Délèze, S. Drissi, P. Garrett, J. Jolie, J. Kern, S. Mannanal, and J. P. Vorlet, Proc. 8th Int. Symposium on Capture gamma-ray spectroscopy and related topics, Fribourg (Switzerland) 1993, edited by J. Kern (World Scientific, Singapore, 1994) p. 314.
[33] U. Kneissl, H. H. Pitz, and A. Zilges, Prog. Part. Nucl. Phys. **37**, 349 (1996).
[34] U. E. P. Berg and U. Kneissl, Annu. Rev. Nucl. Part. Sci. **37**, 33 (1987).
[35] W. Andrejtscheff, C. Kohstall, P. von Brentano, C. Fransen, U. Kneissl, N. Pietralla, and H. H. Pitz, Phys. Lett. **B506**, 239 (2001).
[36] J. Bryssinck, L. Govor, D. Belic, F. Bauwens, O. Beck, P. von Brentano, D. De Frenne, T. Eckert, C. Fransen, K. Govaert, R.-D. Herzberg, E. Jacobs, U. Kneissl, H. Maser, A. Nord, N. Pietralla, H. H. Pitz, V. Yu. Ponomarov, and V. Werner, Phys. Rev. C **59**, 1930 (1999).
[37] N. Pietralla, C. Fransen, D. Belic, P. von Brentano, C. FrieBner, U. Kneissl, A. Linnemann, A. Nord, H. H. Pitz, T. Otsuka, I. Schneider, V. Werner, and I. Wiedenhöver, Phys. Rev. Lett. **83**, 1303 (1999).
[38] V. Werner, D. Belic, P. von Brentano, C. Fransen, A. Gade, H. von Garrel, J. Jolie, U. Kneissl, C. Kohstall, A. Linnemann, A. F. Lisetskiy, N. Pietralla, H. H. Pitz, M. Scheck, K.-H. Speidel, F. Stedile, and S. W. Yates, Phys. Lett. **B550**, 140 (2002).
[39] C. Fransen, N. Pietralla, A. P. Tonchev, M. W. Ahmed, J. Chen, G. Feldman, U. Kneissl, J. Li, V. Litvinenko, B. Perdue, I. V. Pinayev, H. H. Pitz, R. Prior, K. Sabourov, M. Spraker, W. Tornow, H. R. Weller, V. Werner, Y. K. Wu, and S. W. Yates, Phys. Rev. C **70**, 044317 (2004).
[40] N. Pietralla, C. J. Barton III, R. Krücken, C. W. Beausang, M. A. Caprio, R. F. Casten, J. R. Cooper, A. A. Hecht, H. Newman, J. R. Novak, and N. V. Zamfir, Phys. Rev. C **64**, 031301(R) (2001).
[41] C. Fransen, N. Pietralla, Z. Ammar, D. Bandyopadhyay, N. Boukharouba, P. von Brentano, A. Dewald, J. Gableske, A. Gade, J. Jolie, U. Kneissl, S. R. Lesher, A. F. Lisetskiy, M. T. McEllistrem, M. Merrick, H. H. Pitz, N. Warr, V. Werner, and S. W. Yates, Phys. Rev. C **67**, 024307 (2003).
[42] A. Gade, D. Belic, P. von Brentano, C. Fransen, H. von Garrel, J. Jolie, U. Kneissl, C. Kohstall, A. Linnemann, H. H. Pitz, M. Scheck, F. Stedile, and V. Werner, Phys. Rev. C **67**, 034304 (2003).
[43] H. Lehmann, A. Nord, A. E. de Almeida Pinto, O. Beck, J. Besserer, P. vonBrentano, S. Drissi, T. Eckert, R.-D. Herzberg, D. Jäger, J. Jolie, U. Kneissl, J. Margraf, H. Maser, N. Pietralla, and H. H. Pitz, Phys. Rev. C **60**, 024308 (1999).
[44] W. Geiger, Zs. Németh, I. Bauske, P. von Brentano, R. D. Heil, R.-D. Herzberg, U. Kneissl, J. Margraf, H. Maser, N. Pietralla, H. H. Pitz, C. Wesselborg, and A. Zilges, Nucl. Phys. **A580**, 263 (1994).
[45] N. Warr, S. Drissi, P. E. Garrett, J. Jolie, J. Kern, S. J. Mannanal, J.-L. Schenker, and J.-P. Vorlet, Nucl. Phys. **A620**, 127 (1997).
[46] N. Pietralla, I. Bauske, O. Beck, P. von Brentano, W. Geiger, R.-D. Herzberg, U. Kneissl, J. Margraf, H. Maser, H. H. Pitz, and A. Zilges, Phys. Rev. C **51**, 1021 (1995).
[47] B. Schlitt, U. Maier, H. Friedrichs, S. Albers, I. Bauske, P. von Brentano, R. D. Heil, R.-D. Herzberg, U. Kneissl, J. Margraf, H. H. Pitz, C. Wesselborg, and A. Zilges, Nucl. Instrum. Methods Phys. Res. A **337**, 416 (1994).
[48] H. Maser, S. Lindenstruth, I. Bauske, O. Beck, P. von Brentano, T. Eckert, H. Friedrichs, R. D. Heil, R.-D. Herzberg, A. Jung, U. Kneissl, J. Margraf, N. Pietralla, H. H. Pitz, C. Wesselborg, and A. Zilges, Phys. Rev. C **53**, 2749 (1996).
[49] J. Margraf, T. Eckert, M. Rittner, I. Bauske, O. Beck, U. Kneissl, H. Maser, H. H. Pitz, A. Schiller, P. vonBrentano, R. Fischer, R.-D. Herzberg, N. Pietralla, A. Zilges, and H. Friedrichs, Phys. Rev. C **52**, 2429 (1995).
[50] N. Pietralla, P. von Brentano, R.-D. Herzberg, U. Kneissl, N. Lo Iudice, H. Maser, H. H. Pitz, and A. Zilges, Phys. Rev. C **58**, 184 (1998).
[51] J. Enders, P. von Neumann-Cosel, C. Rangacharyulu, and A. Richter, Phys. Rev. C **71**, 014306 (2005).

[52] P. van Isacker, K. Heyde, J. Jolie, and A. Sevrin, Ann. Phys. **171**, 253 (1986).
[53] R. Georgi, P. von Neumann-Cosel, T. von Egidy, M. Grinberg, V. A. Khitrov, J. Ott, P. Prokofjevs, A. Richter, W. Schauer, C. Schlegel, R. Schulz, L. J. Simonova, Ch. Stoyanov, A. M. Sukhovoj, and A. V. Vojnov, Phys. Lett. **B351**, 82 (1995).
[54] R. Schwengner, G. Winter, W. Schauer, M. Grinberg, F. Becker, P. von Brentano, J. Eberth, J. Enders, T. von Egidy, R.-D. Herzberg, N. Huxel, L. Käubler, P. von Neumann-Cosel, N. Nicolay, J. Ott, N. Pietralla, H. Prade, S. Raman, J. Reif, A. Richter, C. Schlegel, H. Schnare, T. Sevene, S. Skoda, T. Steinhardt, C. Stoyanov, H. G. Thomas, I. Wiedenhöver, and A. Zilges, Nucl. Phys. **A620**, 277 (1997).
[55] V. Yu. Ponomarev, Ch. Stoyanov, N. Tsoneva, and M. Grinberg, Nucl. Phys. **A635**, 470 (1998).
[56] R. V. Jolos and W. Scheid, Phys. Rev. C **66**, 044303 (2002).
[57] R. V. Jolos, N. Yu. Shirikova, and V. V. Voronov, Phys. Rev. C **70**, 054303 (2004).
[58] A. Bohr and B. Mottelson, Nucl. Phys. **4**, 529 (1957); **9**, 687 (1959).
[59] V. Strutinsky, J. Nucl. Energy **4**, 523 (1957).
[60] S. Raman, C. W. Nestor, and P. Tikkanen, At. Data Nucl. Data Tables **78**, 1 (2001).
[61] T. Kibédi and R. H. Spear, At. Data Nucl. Data Tables **80**, 35 (2002).
[62] M. Babilon, diploma thesis, TU-Darmstadt (2001), unpublished.
[63] T. Hartmann, J. Enders, P. Mohr, K. Vogt, S. Volz, and A. Zilges, Phys. Rev. Lett. **85**, 274 (2000).
[64] M. Babilon, T. Hartmann, P. Mohr, K. Vogt, S. Volz, and A. Zilges, Phys. Rev. C **65**, 037303 (2002).
[65] F. Iachello, Phys. Lett. **B160**, 1 (1985).
[66] C. Kohstall, Dissertation, University of Stuttgart 2004, unpublished.
[67] A. Bohr and B. R. Mottelson, *Nuclear Structure* Vol. II (Benjamin, New York, 1975).
[68] V. Yu. Ponomarev, C. Stoyanov, N. Tsoneva, and M. Grinberg, Nucl. Phys. **A635**, 470 (1998).
[69] V. Yu. Ponomarev, J. Bryssinck, L. Govor, F. Bauwens, O. Beck, D. Belic, P. von Brentano, D. De Frenne, C. Fransen, R.-D. Herzberg, E. Jacobs, U. Kneissl, H. Maser, A. Nord, N. Pietralla, H. H. Pitz, and V. Werner, Phys. Rev. Lett. **83**, 4029 (1999).
[70] J. Bryssinck, L. Govor, V. Y. Ponomarev, F. Bauwens, O. Beck, D. Belic, P. von Brentano, D. De Frenne, C. Fransen, R.-D. Herzberg, E. Jacobs, U. Kneissl, H. Maser, A. Nord, N. Pietralla, H. H. Pitz, and V. Werner, Phys. Rev. C **62**, 014303 (2000).
[71] J. Bryssinck, L. Govor, F. Bauwens, D. Belic, P. von Brentano, D. De Frenne, C. Fransen, A. Gade, E. Jacobs, U. Kneissl, C. Kohstall, A. Linnemann, A. Nord, N. Pietralla, H. H. Pitz, M. Scheck, F. Stedile, and V. Werner, Phys. Rev. C **65**, 024313 (2002).
[72] M. Scheck, H. vonGarrel, N. Tsoneva, D. Belic, P. von Brentano, C. Fransen, A. Gade, J. Jolie, U. Kneissl, C. Kohstall, A. Linnemann, A. Nord, N. Pietralla, H. H. Pitz, F. Stedile, C. Stoyanov, and V. Werner, Phys. Rev. C **70**, 044319 (2004).
[73] A. Nord, J. Enders, A. E. de Almeida Pinto, D. Belic, P. von Brentano, C. Fransen, U. Kneissl, C. Kohstall, A. Linnemann, P. von Neumann-Cosel, N. Pietralla, H. H. Pitz, A. Richter, F. Stedile, and V. Werner, Phys. Rev. C **67**, 034307 (2003).